

## 9. MICROFACIES AND MICROFABRICS OF EARLY MIDDLE CRETACEOUS SEDIMENTS SELECTED FROM SITE 370, DSDP LEG 41 (DEEP BASIN OFF MOROCCO)

Diethard E. Meyer, Fachbereich 9 der Universität Essen, D-4300 Essen, Germany

### ABSTRACT

Preliminary results in this paper concern 10 samples selected from mid-Cretaceous sediments from Leg 41, DSDP Site 370 off the Moroccan continental margin (northwest Africa). These samples originate from a subbottom depth of more than 835 meters. They represent interbeds of relatively coarse-grained lithified sediments including quartz-bearing calcirudites, calcarenites, and calcisiltites, in a sequence of predominantly silty and nanno-bearing shales of late Neocomian to lower Aptian age.

The microfacies and microfabrics of the samples have been studied by optical and scanning electron microscope as well as by X-ray diffraction, chemical, and staining methods. Different microfacies types (A-E) were distinguished according to specific composition. They are abundant, especially quartz, potassium feldspar, plagioclase, dolomite, and fragments of polygenetic rocks. Furthermore, the sediments include allochemical components that have originated in shallow-water environments. These components are mainly biogenic detritus, as well as oolites, superficially coated grains, and glauconite particles. Probably most of the coarse material was transported by turbidity currents from shelf and continental sources into the basin. The arenaceous sediments are well cemented grainstones in which up to three sequences of calcite cement can be differentiated.

### INTRODUCTION

This study deals with the analysis of 10 samples of Early Middle Cretaceous age from Site 370, Leg 41, located off northwest Africa (Eastern North Atlantic). The samples consist of different types of clay-, silt-, sand-, and gravel-sized lithified sediments. There are two main points of general interest: first, the character and origin of the terrigenous and bioclastic components, and second, the problem of cementation.

Site 370 is located in the southern part of the basin off the Moroccan continental margin at 32°50.2'N and 10°46.6'W, about 155 km northwest of Safi. The water depth is 4214 meters. The samples were selected from Cores 32 and 34 in a nearly 50-meter-thick sequence of late Neocomian to lower Aptian age sediments. Silty and nanno-bearing shales predominate. The shales are intercalated by layers of argillaceous or calcareous siltstones, arenaceous limestones, and conglomerates. The recovered sediments directly above and below the shale sequence consist predominantly of nanno-bearing claystones alternating with silty claystones (Core 31), and nanno marlstones interbedded with silty clay (Core 35).

### PROCEDURES

Ten samples were selected by E. Seibold. Most of the samples from Cores 32 and 34 are lithified carbonate sediments. Rock slabs measuring a few square centimeters in area and 5-8 mm in thickness were cut normal to bedding.

Reconnaissance studies were made with a binocular microscope on freshly fractured surfaces. Small pieces (60-120 mg) were split off and chemically analyzed. The rock slabs were superficially impregnated by araldite, polished and photographed in order to document sedimentary structures. Pyrite-rich samples were studied under reflected light with a Zeiss Ultraphot II microscope. X-radiographs were made of 3-5 mm thick slices of the samples for textural information.

Mineral constituents were determined by X-ray diffraction analyses of untreated dry powder specimens using a Philips diffractometer (Cu K $\alpha$  radiation, LiF monochromator, 1° (per minute scanning speed). The pelitic specimen (Sample 370-32-4, 25-28 cm) was treated with diethylene glycol and submitted to X-ray diffraction. This sample was also submitted to differential thermal analysis (20-980°C, receiv. 0.3 mv, 10°C per minute speed).

Microfacies and microfabrics were studied on thin sections covering the size of the sample. In order to differentiate non-ferroan and ferroan calcite generations, thin sections of carbonate sediments were partially etched and stained with Alizarin red-S and potassium ferricyanide in diluted hydrochloric acid (Lindholm and Finkelman, 1972). Quantitative determination was made on the basis of point counts on thin-sections in transmitted light. Grain-size distribution determined in thin section was based upon the projected area diameter; a Zeiss grain size stage was used. Microfabrics and qualitative elementary distribution were examined in carbon-coated samples

with a Cambridge S4 scanning electron microscope, coupled with energy-dispersive X-ray analyzer Ortec, 6200.

### CLASSIFICATION

The following samples have been studied:

Core 32, 834.5 to 844.0 meters subbottom depth—370-32-2, 52-55 cm; 370-32-3, 12-16 cm; 370-32-3, 47-48 cm; 370-32-4, 25-28 cm; 370-32-4, 86-89 cm; 370-32-4, 118-122 cm.

Core 34, 872.5 to 882.0 meters subbottom depth—370-34-1, 46-48 cm; 370-34-1, 68-71 cm; 370-34-1, 77-79 cm; 370-34-4, 113-116 cm.

In the different rock types, grain-size distribution varies from silt to pebble size. Typically the sediments are cemented by sparry calcite and do not have a clayey matrix.

The following main types of sediments, which include the microfacies types A-E can be differentiated:

- 1) Silty carbonate-free shale (semilithified pelite): Sample 370-32-4, 25-28 cm.
- 2) Silty calcareous shales: Sample 370-32-3, 12-16 cm; Sample 370-32-3, 47-48 cm.
- 3) Silty quartz-bearing limestone (calcsiltite): (A) Sample 370-34-4, 113-116 cm.
- 4) Arenaceous quartz-bearing limestones (calcarenites): (B) Sample 370-32-2, 52-55 cm; (C) Sample 370-34-1, 77-79 cm; (D1) Sample 370-34-1, 68-71 cm; (D2) Sample 370-34-1, 46-48 cm.
- 5) Conglomeratic quartz-bearing carbonates (calcirudites): (E1) Sample 370-32-4, 86-89 cm; (E2) Sample 370-32-4, 118-122 cm.

### MINERAL COMPOSITION

#### Terrigenous Components

All samples contain varying portions of terrigenous detritus. Quartz, a minor constituent (5%-25%), is apparently the most abundant of the terrigenous components. In silt- and sand-size fractions quartz grains are highly variable in shape, roundness, and surface character; are mostly clear, colorless, or milky; and are occasionally reddish. Euhedral quartz crystals occur rarely. The great variety of mono- and polycrystalline quartz is mainly represented by fragments of quartz-rich rocks of sedimentary, igneous, and metamorphic origin. In all samples the ratio of K-feldspar/plagioclase is high (about 10:1 or more). Most of the K-feldspar grains (microcline, orthoclase, perthite) are partially sericitized. Muscovite, mica-illite, glauconite, and biotite (very rare) were recognized. In addition, the pelitic fraction with increased mica content also contains kaolinite and traces of chlorite. Accessory constituents of terrigenous origin are dolomite (coated grains), tourmaline, rounded zircon, rutile, sphene (?), apatite, and garnet.

In the coarse fractions of arenaceous and conglomeratic layers, rock erosion fragments are frequent. In general the lithoclastic components are angular or subangular to well rounded. Quartz aggregates (metaquartzite, polycrystalline, and sutured quartz, chert?) are most abundant as well as silicate-rich rock particles (quartz-feldspar aggregates, volcanic rocks

with microlites, carbonaceous quartzites, sandstones, and siltstones). These rock fragments, which occur mainly in the arenaceous limestones, must be derived primarily from crystalline plutonic-metamorphic sources. Volcanic rock fragments and volcanic glass are rare. Large lithic fragments dominate in the conglomerate (Sample 370-32-4, 118-122 cm), in which mostly rounded fragments of fine to microcrystalline carbonates are abundant (Ca-dolomites, argillaceous limestones, quartz-bearing limestones, and dolomites).

#### Biogenous Components

Biogenous components occur in variable percentages as most samples: scattered fossil tests (foraminifers, calcispheres, ?radiolarians), algal detritus, skeletal remains (mollusks, brachiopods), fish and plant debris. Most of these fossil remains consist of calcite (originally low- and high-magnesian calcites) or aragonite which is partly preserved. On the other hand, non-carbonate biogenic particles (phosphatic carbonaceous) may be enriched in thin layers. The relatively small bioclastic grains are often coated by concentric layers of calcite whereas the larger skeletal elements may be diagenetically altered (micritic rims, neomorphic spar, pyritization).

#### Authigenic Constituents

The group of minerals formed by diagenetic processes includes mainly carbonates as overgrowth and drusy cement (calcite, ferroan calcite, partially ferroan magnesian calcite) as well as products of recrystallization or replacement (calcite, dolomite rhombs). Other authigenic minerals in decreasing frequency: pyrite (replacing fossils, filling casts and voids as framboidal clusters), sericite (alteration product), gypsum, phillipsite, smectite (montmorillonite group), glauconitic minerals and possibly chabasite. Fe/Mn oxides and hydroxides are ubiquitous; they may be locally enriched, e.g., in layers bearing volcanic ash (Sample 370-34-4, 113-116 cm).

### CHEMICAL COMPOSITION

The results of the chemical analyses are listed in Table 1; however, due to the small sample size, the chemical analyses may have restricted significance. This section analysis shows significant differences in the mineralogical composition within the range of a few mm to cm. With respect to mineralogical variations over such small distances chemical analysis may be regarded as characteristic for the overall microfacies sample.

The values of SiO<sub>2</sub> are mainly due to the content of terrigenous quartz. The low content of K and Al can be correlated in most cases with potassium feldspar. Iron is mainly trapped in pyrite. The content of organic carbon is about 1%-3% in most of the samples; but it is extremely low (0.1%) for the greenish almost carbonate-free silty clay of Sample 370-32-4, 25-28 cm. In the coarser grained sediments the organic matter may be concentrated in or around originally porous skeletal remains. Element distribution maps were made for Si, Ca, Mg, Na, K, Al, P, S, Fe, and Ti.

TABLE I  
Chemical Analyses of Early Middle Cretaceous Sediments  
(late Neocomian to lower Aptian) DSDP Leg 41, Site 370, Cores 32 and 34

Sample	32-4, 25-28 cm	32-3, 12-16 cm	32-3, 47-48 cm	34-4, 113-116 cm	32-2, 52-55 cm	34-1, 77-79 cm	34-1, 68-71 cm	32-4, 86-89 cm	32-4 118-122 cm
Microfacies	A				B	C	D1	E1	E2
	Percent								
SiO <sub>2</sub>	65.97	44.10	54.01	21.29	23.97	27.34	14.87	22.34	24.21
Al <sub>2</sub> O <sub>3</sub>	12.62	11.76	5.57	2.50	1.57	1.18	0.92	3.45	3.63
Fe <sub>2</sub> O <sub>3</sub>	3.13	5.51	3.05	1.36	3.37	1.53	1.10	27.00	4.36
FeO	0.94			0.40					
MgO	2.14	2.18	1.24	1.07	1.18	1.31	0.91	2.24	7.27
CaO	0.48	8.29	15.72	39.20	37.31	36.84	45.17	13.49	26.21
SrO	<0.01	0.02	0.02	0.07	0.05	0.07	0.08	0.03	0.03
Na <sub>2</sub> O	1.40	1.19	0.89	0.41	0.69	0.46	0.45	0.63	0.51
K <sub>2</sub> O	3.38	2.90	1.72	0.71	0.70	0.51	0.46	1.05	1.02
TiO <sub>2</sub>	0.93	0.73	0.55	0.27	0.10	0.14	0.11	0.32	0.27
P <sub>2</sub> O <sub>5</sub>	0.17	0.52	0.45	0.16	0.08	0.23	0.11	2.07	0.44
MnO	0.01	0.03	0.03	0.05	0.04	0.03	0.04	0.11	0.14
CO <sub>2</sub>	—	0.32	9.67	28.53	23.93	26.84	33.09	3.21	22.18
C	0.10	6.16	1.71	1.06	2.07	0.74	1.08	2.89	1.87
H <sub>2</sub> O	≤ 9.89	≤ 13.65	≤ 4.09	1.92	1.62	1.54	1.53	4.50	3.81
SO <sub>3</sub>	0.32	3.75	2.18	1.37	3.35	1.76	—	16.21	4.02

Note: Analyst: T. Kost.

## MICROFACIES AND PETROGRAPHY

### Microfacies A

Occurrence: 370-34-4, 113-116 cm. Age: Neocomian (upper Hauterivian?). Size of specimen: 2.1 × 2.25 × 0.5 cm (2.4 cm<sup>3</sup>).

The sorted silty quartz biosparite is rhythmically thin bedded. Light gray laminae alternate with brownish dark layers (Plate 1, Figure 1). The thickness of the light gray laminae is 0.2-1 mm (maximum 2.2 mm), whereas the dark ferruginous laminae have an average thickness of 0.1-0.5 mm (maximum 1.5 mm). In the specimen 50 light and dark layers per 20 mm of thickness can be differentiated. The radiograph shows faint lamination also in the light colored beds (Plate 1, Figure 2). The light colored laminae are more consistent than the dark ones. Thin sequences of laminae show overturned microfolds (Plate 1, Figure 1), probably due to slumping.

This biosparite consists mainly of 10 μm to 100 μm sized calcite (70%) and a varying content of quartz (<5% up to about 10%-15%). The detrital fraction of quartz and feldspar consists of medium- and coarse-grained silt (about 90%) with a median diameter of 5 phi.

According to X-ray determination the amount of potassium feldspar is about 5%. Plagioclase is very rare (<1%); hornblende, biotite, and glauconite (size 40-100 μm) were occasionally noted.

The detrital grains are angular to subangular. The dark colored laminae are characterized by the occurrence of volcanic glass shards and ferruginous minerals. The yellowish brown irregularly shaped glass particles (maximum size 240 μm) bear inclusions of aphanic material.

Euhedral dolomite crystals (10-100 μm in size) are scattered throughout the section. Crystal size of granular mosaic cement (ferroan calcite) ranges from 40 to 280 μm. This type of cement is concentrated in vein-like laminae, especially where microfolding is obvious. Microfossils floating in the groundmass are rare (less than 1%), but in comparison with the microfacies types described below relatively frequent. Most frequent are spheres (65-80 μm) which are partly filled with calcite. Foraminifers as seen in thin section (Plate 2, Figure 4) include planispiral evolute forms as well as biserial tests (100-125 μm in size). The chambers are mostly filled with calcite, or the tests are pyritized. Other skeletal components (maximum size 130 μm) are very rare.

### Microfacies B

Occurrence: 370-32-2, 52-55 cm, Age: late Neocomian (Barremian?) to lower Aptian.

This type is represented by an olive-gray well-cemented limestone which was identified as an arenaceous pyrite- and quartz-bearing bio-ösparite (Plate 1, Figure 3). The grain-supported sediment is not distinctly bedded, and a preferred orientation of the grains is not noticeable. Characteristic for this microfacies is a great variety of allogenic and allochemical constituents. According to their heterogeneous origin the components are highly variable in size, shape, and roundness. At least 25% of the particles are coated grains. Skeletal remains are frequent. The modal composition is listed in Table 2. Grain size varies from coarse sand to silt size.

The total content of terrigenous constituents (mainly quartz, feldspar, siliceous rock fragments) amounts to more than 22%. A high ratio of K-feldspar to

TABLE 2  
Composition (%) of Arenaceous  
Quartz-bearing Limestone  
370-32-2, 52-55 cm (late Neocomian  
to lower Aptian), (1000 points)

Quartz	16.2
Potassium feldspar	1.4
Plagioclase	0.1
Calcite (grains, skeletal remains)	28.6
Calcite (rim cement)	4.9
Ferroan calcite (spar)	36.5
Dolomite	1.2
Pyrite, other opaques	6.2
Heavy minerals	<0.5
Polymineralic grains	4.4
Total	100

plagioclase is characteristic. Grains of quartzite, siliceous and calcareous sandstones, dolomitic carbonates, microcrystalline limestones, and igneous rocks (aplitic rocks, volcanic glass, up to 200  $\mu\text{m}$  in size) occur. The allochemical carbonate constituents include biogenic remains (originally low- and high-Mg calcites, aragonite) and detrital carbonate particles (calcite, dolomite) which amount to more than 30% of the total sample.

Skeletal remains are partially replaced by neomorphic spar (ferroan calcite). In consequence, the proportion of cement-filling interparticle pore space must be lower than the total of ferroan calcite (36%) and of non-ferroan calcitic overgrowth cement (5%), i.e., approximately 41%. On the other hand, the grain volume was determined at 74% (maximum) to 69% (minimum). Thus, the amount of neomorphic ferroan calcite should be in the range of 10%-15%. Thus, one can neglect the volume of microspar (<30  $\mu\text{m}$ ) which can be derived from silt-sized carbonate particles. Generally, the size of precipitated cement and neomorphic spar ranges from 40 to 250  $\mu\text{m}$  (maximum 350  $\mu\text{m}$ ). The size of euhedral dolomite rhombs grown in ferroan calcite cement varies from 10 to 170  $\mu\text{m}$  (30  $\mu\text{m}$  on an average).

Oolites and superficially coated grains are abundant. The cores of these oolitic grains mainly consist of silt- to sand-sized angular grains including quartz, carbonate particles and peloids. The normal thickness of the cortex of most of the oolitic grains ranges between 10-60  $\mu\text{m}$ . The coating on large particles is relatively thin or incomplete.

The biogenic constituents are at least partly well preserved. If one takes into account the partial neomorphic replacement by calcite, the initial content of biogenic components should have exceeded 15%. These remains derive chiefly from echinoderms, mollusca (pelecypods, gastropods), and brachiopoda. Not as frequent are fragments of coralline algae (Plate 2, Figure 5) which are mainly represented by crustose types. Remnants of microfossils (ostracodes, foraminifers) are rare. The echinoderm grains are partially micritic and show borings; many of them show syntaxial overgrowths. They are partly grown up to subhedral crystals (Plate 3, Figure 7). Pyrite (distributed irregularly) may be concentrated in carbonate and skeletal grains. Pyrite fills also intra-particle voids or replaces calcite (Plate 6, Figure 5).

Grain size distribution has been evaluated separately for the terrigenous and allochemical grains (Table 3). The fine and medium sand fractions predominate (about 80%) in both cases. Different distributions are obvious for quartz and carbonate grains in the silt fraction (see Table 3). The absence of carbonate silt is probably caused by the diagenetic formation of microspar. The maximum size of quartz grains is 1.3 mm whereas skeletal remains are up to 2.4 mm in size. Most of the quartz and silicate grains are very angular (12%), angular (32%), and subangular (33%); only 22% are rounded or well rounded (1%).

The grain volume, based on 1500 points on thin section, shows a decrease from 74% in the lower part to 69% in the upper part of the sample, which suggests a relative increase of porosity of about 5%. Taking into account that the effect of compaction was moderate during diagenesis a primary porosity of at least 30% is probable.

### Microfacies C

Occurrence: 370-34-1, 77-79 cm, base of a 40-cm turbidite, underlain by dark greenish shales. Age: late Neocomian (upper Hauterivian — lower Barremian?).

This light greenish gray limestone represents a moderately sorted arenaceous biosparite which is mainly medium to fine grained. This lowermost section of the multigraded turbidite is moderately indurated and, in comparison with specimens from the upper part, relatively porous (compare Microfacies D2); porosity exceeds 5%. Bedding is indistinct. Thus, only a few irregular darkish brown bands (<1 mm) can be seen. Graded bedding is faintly indicated by coarse grains enriched at the base. The carbonate content of the limestone totals to about 70%. The main fabric size is around 10  $\mu\text{m}$ . Coated grains are almost absent, and the ratio of terrigenous components to biogenic constituents is relatively high (about 4:1). The biogenous grains (maximum 7%) are mostly well preserved; foraminifers are very rare.

The composition of the sample is listed in Table 4. The quartz fraction ranges from 15 to 1000  $\mu\text{m}$  and consists predominantly of angular and subangular grains (about 60%), whereas 30% are subrounded and only 10% rounded to well rounded (based on 200 grains

TABLE 3  
Grain-Size Distribution of Transported  
Carbonate and Non-Carbonate  
Grains of Arenaceous Quartz-Bearing  
Limestone 370-32-2, 52-55 cm  
(late Neocomian to lower Aptian) (1000 counts)

	Grain Number		
	Carbonate Grains	Non-Carbonate Grains	
Fine silt	<6 $\phi$	0	2
Medium silt	6-5	0	21
Coarse silt	5-4	2	21
Very fine sand	4-3	89	125
Fine sand	3-2	303	249
Medium sand	2-1	99	76
Coarse sand	1-0	7	6
Very coarse sand	0-1	0	0
Total		500	500

TABLE 4  
Composition (%) of Quartz-Bearing Limestone (Biosparite) from the Base of a Turbidite, 370-34-1, 77-79 cm (late Neocomian) (500 points)

Quartz	20.3
Potassium feldspar	2.0
Plagioclase, anorthoclase	<1
Skeletal carbonate grains (calcite, aragonite)	5.4
Ca-phosphate	<1
Calcite (microspar)	44.6
Calcite (spar > 30 $\mu$ m)	21.0
Dolomite rhombs	<1
Pyrite, other opaques	2.4
Heavy minerals	<1
Polymineral grains	3.1
Visible pores	0.8
Total	100

of coarse silt to sand size). Euhedral quartz crystals as well as grains of typically embayed quartz suggest volcanic sources. Few quartz grains show thin epitaxial overgrowths or crusts of quartz or ?chalcedony; other grains show highly corroded surface textures (Plate 4, Figure 1). Feldspar (potassium feldspar, plagioclase, ?anorthoclase) occurs as angular to subangular grains up to 750  $\mu$ m in size. Lithic grains are rare. Fragments of partly micron-sized carbonates (up to 1.2 mm), of meta-quartzites and chalcidonic quartz occur. Pyrite forms are irregular to well-defined (partly framboidal aggregates); small pyrite crystals were noted in calcitic skeletal remains.

Skeletal grains (up to 1.2 mm) include, in decreasing abundance remains of molluscan shells (mainly pelecypods), echinoderms, brachiopods, algal debris, phosphatic fish debris, and rarely foraminifers (130-250  $\mu$ m). The fabrics of the shell walls (prismatic and nacreous layers) are often well preserved, as shown in scanning electron micrographs. The inner boundaries of vaulted molluscan shell fragments appear mostly sharp when the shelter pores are completely filled by calcite cement. The effect of mechanical compaction is, even on elongated skeletal fragments, of minor importance. Rounded echinoderm grains show clear syntaxial overgrowths up to 60  $\mu$ m thickness (Plate 3, Figure 5).

Grain-size distribution based on a count of 700 non-carbonate particles (mainly quartz) on thin section has shown that the bulk (about 80%) consists of medium and fine sand (1-3 phi); the distribution is skewed to fine sizes. The mean is about 2 $\Phi$ , and sorting is moderate (0.8 phi standard deviation). The length-to-width ratio was determined for the coarsest fractions (350-1000  $\mu$ m) of terrigenous and biogenic constituents. For quartz, feldspar, and lithic grains this ratio is in the range of 1.5 to 3.5; for bioclasts it is generally higher, and ranges mainly from 2.0 to 6.0 (maximum 13). These grains are oriented with their long axes symmetrical to the parting plane, and they are inclined 5°-15° (in both directions) against it.

Interparticle pores are generally filled by drusy calcite cement (crystal size 25-150  $\mu$ m); only very large

pores (e.g., shelter pores) may be filled by spar up to 650  $\mu$ m. Occasionally, tiny rhombs of dolomite float in sparry calcite. The existence of different nucleation centers is indicated by spar with rather indistinct boundaries and many inclusions (e.g., quartz, pyrite). Aggregates of zeolites may fill remaining pores.

#### Microfacies D1

Occurrence: 370-34-1, 68-71 cm, from the lower part of a 40-cm turbidite, situated about 10 cm from the base. Age: late Neocomian (upper Hauterivian—lower Barremian?).

The light greenish gray arenaceous limestone (Plate 1, Figure 4) represents a moderately well sorted quartz-bearing bio-oösparite (very fine to medium sand). This calcarenite is a well cemented grainstone of which the carbonate content totals 86%. In the uppermost portion of the 3.6 cm thick layer the oösparitic limestone grades into a finely crystalline limestone, which is almost bare of quartz and oöids. This thin layer (3-4 mm thick) is cut by white drusy calcite forming the uppermost part (2 mm) of the sample (Plate 3, Figure 2). There is no sharp boundary between the oösparite representing microfacies D1 and the microsequence following above. The contact between this microsequence and the drusy calcite is faintly undulating, but subparallel to bedding.

The depositional texture of the oölitic limestone is characterized by straight orientation of elongated to flaky grains (mainly bioclasts, up to 1.9 mm). The long axes of the grains are inclined up to 10°-15° relative to the bedding plane, with the exception of the base of the section where clear imbrication is not noticeable.

Typical for this microfacies is the abundance of allochemical components: coated grains, skeletal remains (chiefly echinoderm and molluscan fragments), and non-skeletal components (aggregates, lumps). Most of the quartz grains are coated. The composition has been determined separately for the lower and the upper part of the thin section (Table 5). Only a few grains of plagioclase and a restricted number of rock fragments (cemented sandstone, [?]chert, microlitic volcanics) occur. The content of pyrite is very low. Authigenic dolomite crystals (5-50  $\mu$ m) are very rare.

The coated grains (25%-30%) are well-developed oöids and superficially coated particles (up to 160  $\mu$ m) and the coatings are up to 50  $\mu$ m thick (Plate 5, Figure 6). Large platy skeletal fragments may be thinly coated. In general, the core of the oörites consist of variably shaped ovoid to spherical carbonate particles (calcite, dolomite) and of quartz grains. The detrital dolomite grains occur mostly in the form of angular to subangular grains with partly abraded corners. The skeletal components (predominantly <500  $\mu$ m) include remnants of echinoderms (echinoids, crinoids), pelecypods, brachiopods, coralline algae(?) and rarely foraminifera. Many of the components show borings and micritization (Plate 2, Figure 2). The relatively frequent echinoderm grains have syntaxial overgrowths. Oörites may be broken and filled by ferroan calcite; thin flaky skeletal remains are rarely broken by compactive pressure. Composite non-skeletal grains

TABLE 5  
Composition (%) of Quartz-Bearing Limestone  
from About 10 cm above the Base of a Turbidite,  
370-34-1, 68-71 cm (late Neocomian),  
(1000 points in the lower part and 750 points  
in the upper part of thin section)

	Lower Part	Upper Part
Quartz	7.9	6.9
Potassium feldspar	1.1	1.3
Plagioclase	0	0.1
Dolomite (detrital grains)	1.3	0.9
Calcite		
(bioclasts, coated grains)	37.9	38.8
Calcite (overgrowth)	5.4	10.3
Ferroan calcite		
(cement, neomorphic spar)	41.6	36.5
Opaques and pyrite	1.2	2.0
Heavy minerals	0.3	0.3
Polymineral grains		
(lithic grains, aggregates)	3.3	2.8
Total	100	100

(lumps and aggregates) show carbonate and quartz grains jointed by a brownish cryptocrystalline carbonate matrix.

Grain-size distribution based on terrigenous components counted in thin section (1500 grains) suggests faint graded bedding. The fraction of fine to medium sand decreases from the base to the top by almost 10%, from about 80% to 70%. The proportion of very fine sand to medium silt increases resulting in the size mean changing from 2.3 to 2.6 phi.

The drusy mosaic cement of the second generation (ferroan calcite) is 30 to 200  $\mu\text{m}$  in size. Intraparticle voids and fractures, also in grain size dimensions, are mostly filled with drusy ferroan calcite cement which follows a first-stage cement of non-ferroan calcite. Echinoderm particles may show both types in the form of syntaxial overgrowth. Single calcite grains show polysynthetic twinning in both grain and overgrowth. At the top of the sample is a section of polysynthetically twinned drusy calcite. The crystals of this calcite are grown up more or less vertically on the microsparite substrate, which probably forms the base of a cm-wide tabular vug. Crystal size increases upwards due to competitive growth (Plate 3, Figure 2).

### Microfacies D2

Occurrence: 370-34-1, 46-48 cm from the uppermost section of a 40-cm turbidite. Age: late Neocomian (upper Hauterivian—lower Barremian?).

The light gray arenaceous limestone is classified as a fine-grained medium sand- to silt-sized quartz-bearing bio-oösparite which is very well indurated. The porosity is low; disaggregation of the oölitic limestone is difficult. In the sample range (2.6 cm thickness) the limestone shows a rather uniform texture, as there is neither change of material nor graded bedding. The long axes of bioclasts (up to 1.0 mm) may indicate bedding, whereas other grains are oriented vertically. The sediment is moderately well sorted (standard deviation 0.5 phi), the fine sand fraction being

abundant (70%) and the mean ranging at about 2.5 phi. Grain-size distribution suggests a mixture of two different distributions.

The microfacies is characterized by coated grains (35%-40%) and partly coated skeletal remains (about 10%). The total amount of quartz, feldspar, and lithic grains does not exceed 10%. The modal composition is listed in Table 6. The coated grains are oölitic (up to 200  $\mu\text{m}$ ) with irregular-shaped cores, or they are grains showing superficial coating with few or incomplete lamellae pointing to interruptions during oölitic growth. The nuclei consist mainly of carbonate particles (calcite, dolomite) of skeletal or non-skeletal origin, but cores consist also of quartz, feldspar, and lithic grains (quartzose limestones, quartzites, quartz-bearing and pure dolomites).

The carbonate particles, when coated, appear mostly subrounded to rounded in shape. In contrast, the grains without coating are commonly angular to subangular. Coated grains of potassium feldspar show partially disintegrated rims which probably originated prior to coating. Crystal fragments of dolomite show partly abraded corners or are coated; these grains must be considered detrital. Tiny dolomite rhombs scattered in ferroan calcite cement are authigenic.

The biogenous constituents are primarily broken skeletal remains of mollusca (pelecypods, cephalopods), echinoderms, calcareous algae, and fishes. Only a few poorly preserved foraminifers were found. The smaller skeletal grains are generally better rounded than larger remains (up to 3 mm). Shell structures are often well preserved. Thus, large prisms of calcite may represent the outer prismatic layer of Pinnacea (Plate 5, Figure 1). Nacreous (aragonitic) layers have been recognized by SEM.

The framework of the grainstones is almost completely cemented by two different types of calcite cement. Low-magnesian calcite is abundant (main size, tens of  $\mu\text{m}$ ), whereas the amount of ferroan calcite (mainly 25-200  $\mu\text{m}$ ) is relatively low. In accordance with mesogenetic conditions the ferroan calcite cement occurs in interparticle pore space. Intraparticle pores (up to 200  $\mu\text{m}$ ) may be completely filled by microspar. It remains uncertain whether the ferroan calcite occurring in the cores of coated grains has been formed by neomorphic process or not.

TABLE 6  
Composition (%) of Quartz-Bearing  
Limestone (Bio-oösparite)  
from the Uppermost Part of a  
Turbidite, 370-34-1, 46-48 cm  
(late Neocomian) (1000 points)

Quartz	6.9
Potassium feldspar	0.5
Dolomite (detrital grains)	1.1
Non-ferroan calcite	71.2
Ferroan calcite (spar)	15.0
Lithic and polymineral grains	3.6
Pyrite, other opaques	0.9
Non-identified minerals	0.8
Heavy minerals	<1
Total	100

Elementary distribution maps are in accordance with the low Mg-content indicated by X-ray analysis (bulk sample: approximately 2.5 mole %  $\text{MgCO}_3$ ). Ferroan calcite cement has probably slightly elevated Mg-values. Spot analysis has shown significant differences of Mg-content of carbonate particles, shell material, oölitic coatings, and cement. In this example (Plate 5, Figure 5), the allochemical constituents show values of 2-3 mole %  $\text{MgCO}_3$ ; the values of the coating are in the same range. In contrast, the non-ferroan calcite cement is relatively poor in magnesium (less than 2.5 mole %  $\text{MgCO}_3$ ). In the coatings Al and Si are enriched. Concentrations of Fe are generally due to pyrite. On the other hand, iron is present with K, Al, and Si revealing K-feldspar.

### Microfacies E1

Occurrence: 370-32-4, 86-89 cm. Rudaceous layer intercalated in silty shales about 30 cm above the top of a conglomerate (see Microfacies E2). Age: upper Neocomian (Barremian?) to lower Aptian.

The dark gravelly thin bed representing 1.7 cm of the sample is pyrite rich. Although the sediment is lithified, disaggregation is not difficult. A thin layer rich in plant debris separates the relatively coarse-grained lower bed, designated as this microfacies type, from a finer grained dark greenish colored layer forming the upper part of the sample. The pyrite-rich rudaceous sediment of the lower part is poorly sorted and shows a grain-size distribution varying from medium sand to granule size with the largest bioclastic fragments measuring about 5 mm (Plate 1, Figure 6). The indistinctly bedded layer contains allochemical and detrital grains of highly variable shape; a clayey silica matrix is absent. The rock is cemented by calcite and pyrite.

There are the following main mineral constituents according to X-ray and thin section analysis: calcite (approximately 30%), dolomite (25%-30%), quartz (10%-15%), and pyrite (about 10%). Minor constituents are potassium feldspar, Ca-phosphates, illite, plagioclase, zeolites, glauconitic grains, tourmaline, and ?garnet. In this case, the result of the chemical analysis subsample is apparently not representative of the overall sample because of heterogeneity.

Characteristic of this microfacies is the high proportion of angular to subrounded rock fragments in which detrital grains of partly micritic limestones, dolomites, and quartzose dolomites are most abundant; less frequent are silt-bearing argillaceous rocks and chert. Of special interest are intraclasts consisting mainly of pyrite, with few grains of quartz ( $<100 \mu\text{m}$ ) included. Grains of igneous rocks (e.g., aplitic), volcanic glass (in form of spherical yellowish brown particles up to  $800 \mu\text{m}$ ) and botryoidal aggregates of chalcedony are rare.

Most of the skeletal components consist of calcium carbonates (partly low-Mg calcite), phosphates, and carbonaceous matter. The bioclasts include mainly molluscan, echinoderm, fish and plant remains. Echinoderm grains show serrated syntaxial rims. Microfossil remains are rare and poorly preserved. The interior of biogenous remains or originally hollow fossil tests may be filled by framboidal pyrite. In one case the

size of pyrite spherules increases from the wall to the interior (Plate 2, Figure 3). However, for most of the clusters of framboidal pyrite occurring in the intercrystal pores (Plate 5, Figure 3), there is no direct connection with biogenic remains. The size of these authigenic pyrite spherules is wide-ranging ( $5\text{-}300 \mu\text{m}$ ).

Typical for this rock type are the microfabrics of cement consisting of interlocked euhedral calcite crystals (Plate 4, Figure 3). This calcite (Plate 4, Figure 4) was identified as a ferroan magnesian calcite ( $5\text{-}35 \mu\text{m}$ ) with probably more than 5 mole %  $\text{MgCO}_3$ . Similar rhombohedral crystals ( $20\text{-}35 \mu\text{m}$ ) showing relatively high content of Al, Fe, Ca, Si, S, K, and traces of Cu may be related to chabasite. Dolomite rhombs ( $20\text{-}80 \mu\text{m}$ ) are rare. Intraparticle cells of fish debris occur with calcite crystals (Plate 2, Figure 6). Other biogenic fragments fractured by compaction pressure are healed with calcite cement, the fracture planes appearing sharp and not corroded. On the other hand, calcite cement crystals may show corroded texture due to replacing pyrite that forms cement-like masses.

### Microfacies E2

Occurrence: 370-32-4, 118-122 cm from the conglomerate between 116-123 cm, near the base of the lowermost section of Core 32. Age: upper Neocomian (Barremian?) to lower Aptian.

The conglomerate is classified as zeolite-, pyrite-, and quartz-bearing calcirudite. Polymictic rock fragments of granule to pebble size, up to 6 mm in diameter, characterize this coarse moderately indurated sediment which is intercalated in silty shales. A preferred orientation of the light to dark colored grains is not evident with the exception of platy bioclasts which tend to be oriented more or less parallel to bedding (Plate 1, Figure 5). The interstices of the grain-supported framework are filled by a mud-bearing greenish gray calcareous matrix. The mineral constituents are calcite, dolomite, quartz, pyrite, mica-illite, phillipsite, gypsum, and potassium feldspar. Calcite is more abundant than dolomite. The total carbonate content is about 60%. Quartz does not exceed 10%. Preliminary results concerning the specific composition of the rock fragments prove that most of the subrounded to well-rounded components originate from preexisting rocks. These are predominantly light to yellowish brown finely crystalline pure dolomites, quartz-bearing dolomites, and micritic to microsparitic limestones (partly foram bearing). The dolomites show Ca excess, and their composition varies from  $\text{Ca}_{53}\text{Mg}_{47}(\text{CO}_3)_2$ , up to  $\text{Ca}_{55}\text{Mg}_{45}(\text{CO}_3)_2$ , according to the diagram given by Goldsmith, Graf and Joensuu (1955). Typical is a low degree of ordering (0.4-0.5) which is reflected by the ratio  $I(015)/I(110)$ , according to Füchtbauer and Goldschmidt (1965). Grains of polycrystalline quartz and metamorphic quartzite are less abundant. Glauconite grains and large intraclasts consisting of pyrite, with only a few quartz grains occur. Skeletal remains (about 10%) are represented preponderantly by angular to subangular platy molluscan debris (up to 5 mm in length). These fragments may be fractured, due

to compaction although the rate of deformation is moderate. The chemical analysis (see Table 1) is not considered to be representative for the whole sample.

### MICROFABRICS AND CEMENTATION

Here, the grain-to-grain relationships are discussed, chiefly with respect to cementation. Particle size and shape as well as sorting and orientation of the components (see microfacies types A-E) are of great importance, not only for initial arrangement of framework grains and pore space configuration, but also for cementation. As described above, most of the sediments studied are well-cemented grainstones. Tangential contacts are characteristic for almost all those samples in which a clayey silica matrix is practically absent. Typical for the grain-to-grain relations of the randomly packed framework particles is a contact index ranging between 1 and 3. In contrast, long contacts are relatively rare, with the exception of the conglomerate Sample 370-32-4, 118-122 cm. Sutured grains were not noted.

The grain volume of calcarenites and calcirudites, as measured on thin section, indicates relatively high porosity values (at least 30%) and a low rate of compaction. The decrease in initial porosity was mainly affected by cementation of interparticle and intraparticle pore space. Significant intraparticle porosity is related to originally porous biogenic grains (e.g., echinoderms, fish debris), hollow fossil tests (e.g., microfossils), and also to composite grains (aggregates, lumps). The precipitation of calcite cement was initiated by the formation of calcite cement A in the form of short prismatic crystals fringing favored carbonate particles, or in the form of syntaxial rims as shown by echinodermal grains. The formation of cement A must be prior to compactive fracturing of grains, because in no case the fracture planes of crushed biogenous grains show this type of non-ferroan calcite (which is probably a low magnesian calcite). The fracture space is filled by second-stage cement B which is represented by a ferroan calcite. In all cases distinct boundaries between calcite cement A and B were recognized. Most of the interparticle space filling calcite crystals are of cement type B. Nevertheless, the features of cement B appear to be variable in the different microfacies types. Thus, in microfacies type E1 the euhedral cement crystals are Mg-calcite, whereas in other samples the Mg content of the mostly anhedral ferroan calcite seems to be low (<4 mole %  $MgCO_3$ ). The relatively large tabular vug at the top of Sample 370-34-1, 68-71 cm shows elongated calcite crystals grown up competitively from the substrate (Plate 3, Figure 2). This type represents a third generation being almost barren of iron and magnesian.

Geopetal fabrics are not only shown by primary depositional structures (e.g., graded bedding), but also by microfabrics. One of the main indicators for geopetal fabrics in the coarser grained sediments are shelter pores created by elongated components which are often platy bioclasts. These pores are filled by second- and/or third-stage calcite cement.

Fracturing due to compactive stress is practically restricted to large fragments of shells or other biogenic

remains. Apparently the deformation caused by compaction is of minor importance. Sharply bounded fragments of bioclasts are mostly well preserved and occasionally floating in calcite cement. Generally, the angles of deflection shown by crushed skeletal particles are only up to  $10^\circ$ , thus indicating a low compaction rate. Although grain-to-grain movement is not necessarily prevented by the presence of early cement (Bathurst, 1975, p. 465), early cementation with reference to the samples should result in an appreciable preconsolidation effect.

In many cases the differentiation of calcite cement from neomorphic spar is difficult, due to recrystallization. Biogenic and other carbonate grains may be partly replaced by neomorphic calcite as indicated by relict structures. On the other hand, typical *molitic* porosity could not be recognized in the samples. A related texture was noted in only one sample (Plate 1, Figure 3). The type of intercrystalline porosity is of more importance in the case of idiomorphic texture of calcite cement (microfacies E1); here crystal aggregates (zeolites, pyrite) can be found in the intercrystal pores.

### CONCLUSIONS

1. For the relatively coarse-grained sediments of Early Middle Cretaceous age from Cores 32 and 34 (below 835 m subbottom) high ratios of quartz/feldspar and K-feldspar/plagioclase are characteristic. This fact points to similar terrigenous sources. The occurrence of typical shallow-water skeletal debris (which may be coated) together with coated grains of different rock types makes it probable that these materials were brought into the basin from shelf environments. In this connection, it is of much interest that the coarse-grained sandstones and conglomeratic beds of the Barremian/Aptian boundary from the on-land section of Zemzem, located on the African continent about 50 km south east of Essaouira (lat  $34^\circ 16'N$ , long  $9^\circ 20'W$ ), are also characterized by predominance of quartz and potassium feldspar (orthoclase, microcline). In this on-shore section the sources are likely to be situated north of the High Atlas Mountain range. However, a more detailed study is necessary in order to accurately locate the sources of the different rock particles found in the deep sea, off the Moroccan continental margin.

2. The cementation probably began before compactive fracturing of grains in the early stage of diagenesis, as shown by the formation of calcitic overgrowth cement (?low-Mg calcite). Strongly reduced solutions resulted in the precipitation of ferroan calcite which has proved to be at least partially a magnesian calcite. Significant differences in the texture of first- and second-stage calcite cement, and the sharp break between both generations indicate a change in chemical conditions. A third cement generation is indicated by the existence of calcite, which is poor in magnesian and iron. The study of the samples gives no evidence for strong pressure solution. Partial fracturing of elongated grains can be correlated with elevated overburden stress.

## ACKNOWLEDGMENTS

The author gratefully acknowledges E. Seibold (Kiel) for samples and advice, and P. Wurster (Geologisches Institut der Universität, Bonn) for discussion. This work is part of the research program of the Geological Institute, Bonn University. The author is indebted to H.K. Erben (Paleontological Institute, Bonn University) for analytical instrumentation. Thanks are due to all persons who have contributed to this work by comments or technical assistance, mainly to G. Flajs and Mrs. Hemmer. This research was supported by DFG Project Wu32/15-Wu32/16.

## REFERENCES

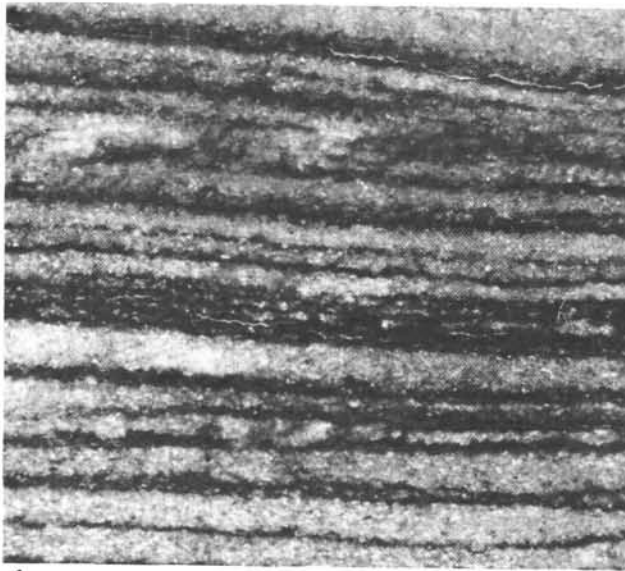
- Bathurst, R.G.C., 1975. Carbonate sediments and their diagenesis, 2nd ed.: Amsterdam, Oxford, New York (Elsevier).
- Füchtbauer, H. and Goldschmidt, H., 1965. Beziehungen zwischen Calciumgehalt und Bildungsbedingungen der Dolomite: Geol. Rundschau, v. 55, p. 29-40.
- Goldsmith, J.R., Graf, D.L., and Joensuu, O.I., 1955. The occurrence of magnesian calcite in nature: Geochim. Cosmochim. Acta, v. 7, p. 212-230.
- Lindholm, R.C. and Finkelman, R.B., 1972. Calcite staining: semiquantitative determination of ferrous iron: J. Sediment. Petrol., v. 42, p. 239-242.

PLATE 1

Sedimentary structures of Site 370 carbonates  
(Cores 32 and 34). All figures show sections  
which are cut normally to bedding and oriented "up."

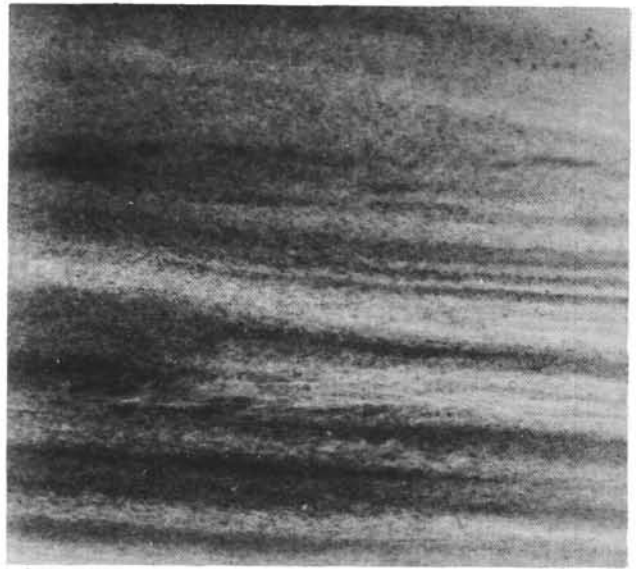
- Figure 1      The finely laminated limestone (microfacies A) shows dark ferruginous laminae alternating with light gray ones. Notice small slump in the upper part of the section (see Figure 2). Photograph of polished surface Sample 370-34-4, 113-166 cm. Reflected light.
- Figure 2      X-radiograph of Figure 1 (congruent section). Sample 370-34-4, 113-116 cm.
- Figure 3      Indistinctly bedded pyrite- and quartz-bearing sparitic limestone (microfacies B) with many coated grains and bioclasts. Note large ovate structure of probably biogenic origin (?mold). Photograph of polished surface Sample 370-32-2, 52-55 cm. Reflected light.
- Figure 4      Moderately well sorted quartz-bearing biosparite (microfacies D 1) with oölitic grains and partly coated bioclasts indicating imbrication. Note vertical fracture which is impregnated by ferruginous compounds. Photograph of polished surface Sample 370-34-1, 68-71 cm. Reflected light.
- Figure 5      Polymictic conglomerate with mud-bearing calcareous matrix (microfacies E 2) showing rounded granules of predominantly finely crystalline carbonates (limestones, dolomites). Note random orientation; some grains are pressure welded. Photograph of polished surface Sample 370-32-4, 118-122 cm. Reflected light.
- Figure 6      Pyrite-rich calcirudite (microfacies E 1) with mostly angular to subrounded rock fragments and bioclasts which may be fractured by compaction. Notice graded bedding. Photograph of polished surface Sample 370-32-4, 86-89 cm. Reflected light.

PLATE 1



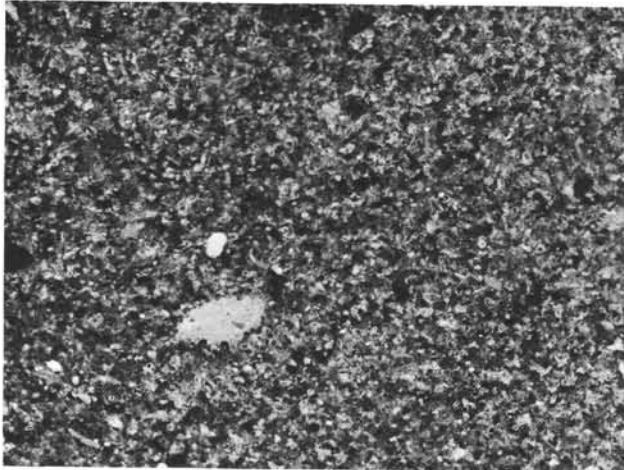
1

2.5 mm



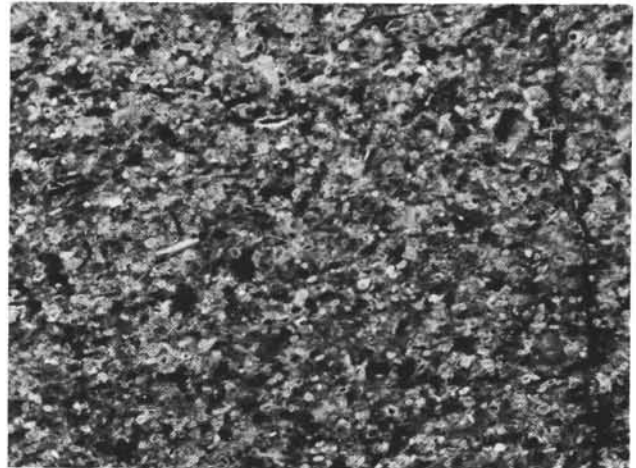
2

2.5 mm



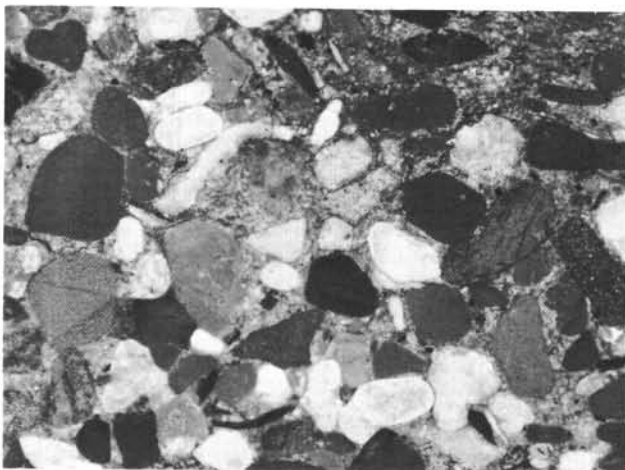
3

2.5 mm



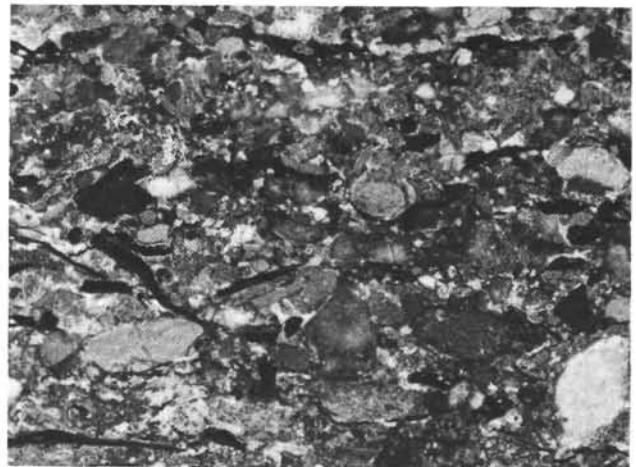
4

2.5 mm



5

2.5 mm



6

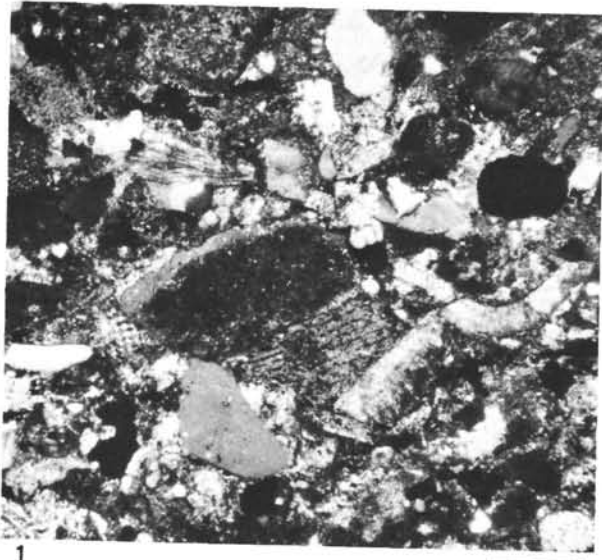
2.5 mm

PLATE 2

Microfacies of limestones from Site 370, Cores 32 and 34,  
and preservation of biogenous constituents.

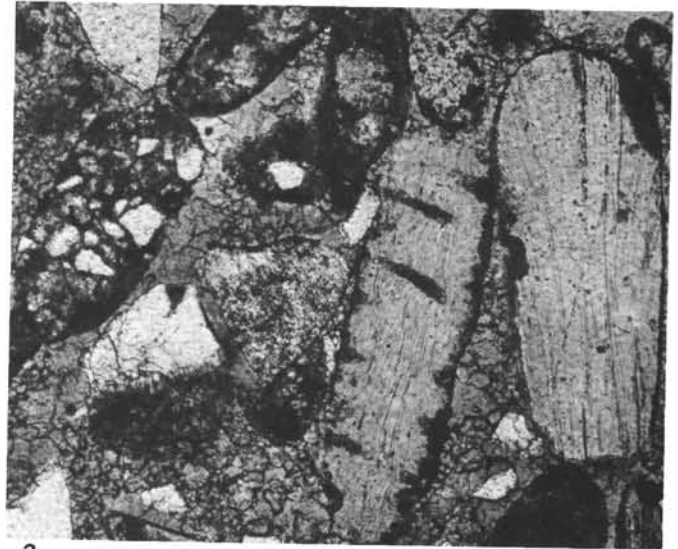
- Figure 1 Echinoderm fragment with dusty interior and syntaxial overgrowth (compare Plate 3, Figure 5), and nearby fossil remains with mainly foliated, radial-fibrous and cellular structures of molluscan and algal origin. Note also rounded to subrounded quartz grains. Thin section Sample 370-34-1, 77-79 cm. Cross-polarized light.
- Figure 2 Molluscan and brachiopod fragments, partially showing micrite envelopes. Note quartzose aggregated grains. Thin section Sample 370-34-1, 68-71 cm, stained with Alizarin red-S and potassium ferricyanide. Plain light.
- Figure 3 Cast of ovate fossil remain filled by framboidal pyrite. Irregular pyrite concentrations outside of the filling. Note pyrite replacing parts of the wall of the remnant. Polished section Sample 370-32-4, 86-89 cm. Reflected light.
- Figure 4 Planispiral foraminifer test (125  $\mu$ m) filled by high-birefringent authigenic mineral. Spherical microfossil of which the lumen is filled by calcite cement. Thin section Sample 370-34-4, 113-116 cm. Plain light.
- Figure 5 Fragment of coralline alga with well-preserved wall structures. Thin section Sample 370-32-2, 52-55 cm, stained with Alizarin red-S and potassium ferricyanide. Plain light.
- Figure 6 Phosphatic fish debris with fibrous structure and interconnected cells which are cemented by large crystals of calcite with different orientation. Thin section Sample 370-32-4, 86-89 cm. Cross-polarized light.

PLATE 2



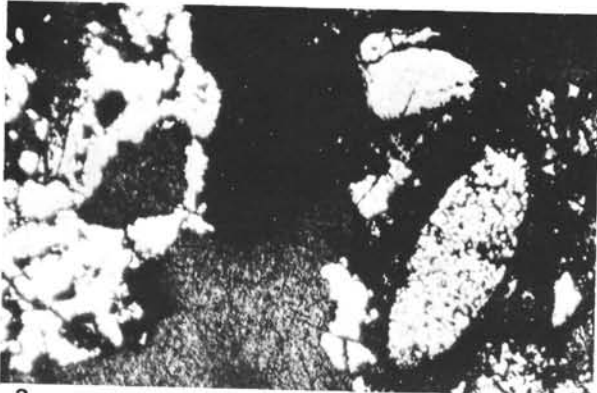
1

250 μm



2

250 μm



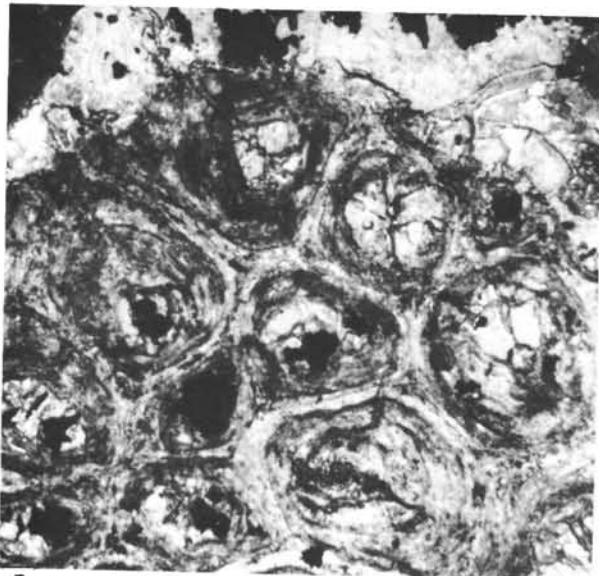
3

250 μm



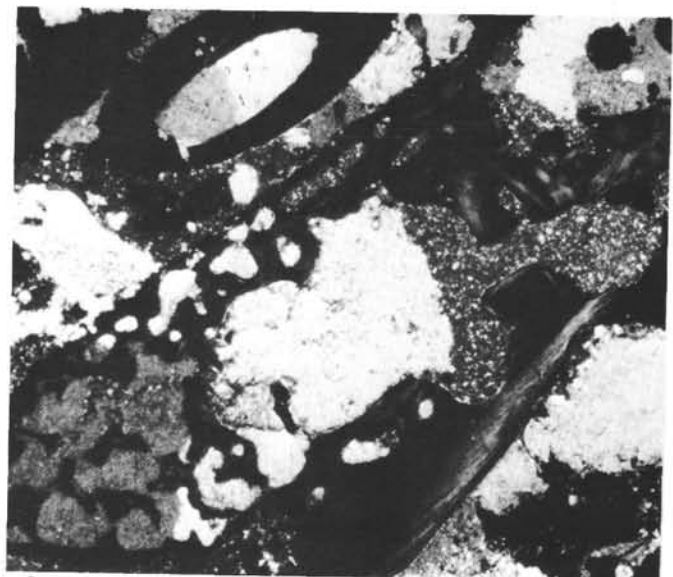
4

50 μm



5

25 μm



6

250 μm

## PLATE 3

Microfacies and cement fabrics of carbonates  
in thin section from Site 370, Cores 32 and 34.

- Figure 1 Cells of a carbonaceous fossil fragment filled with second-generation calcite cement (large crystals exceed cell size) and dusty echinoderm grain with clear syntaxial rim (first generation). Note quartz grain with cracks. Sample 370-32-4, 86-89 cm. Plain light.
- Figure 2 Drusy calcite crystals grown up from the base of an oblong vug; the base consists of almost quartz-free recrystallized calcisiltite. Notice polysynthetic twinning of large calcite crystals. Sample 370-34-1, 68 cm. Cross-polarized light.
- Figure 3 Margin of altered shell fragment fringed by first stage calcite crystals. Interparticle pore space taken by ferroan calcite of second generation. Sample 370-32-2, 52-55 cm, stained with Alizarin red-S and potassium ferricyanide. Plain light.
- Figure 4 Vaulted shell fragment paralleled by first-generation calcite crystals (non-ferroan calcite). Sample 370-32-2, 52-55 cm, stained with Alizarin red-S and potassium ferricyanide. Cross-polarized light.
- Figure 5 Enlargement of Plate 2, Figure 1: partially micritized echinoderm grain with clear syntaxial calcite rim thinning in direction of strongly micritized part. Sample 370-34-1, 78 cm. Cross-polarized light.
- Figure 6 Sparry calcite (?neomorphic) following a vein-like zone subparallel to bedding plane. Notice that quartz content is varying in the different laminae. Sample 370-34-4, 113-116 cm, stained with Alizarin red-S and potassium ferricyanide. Plain light.
- Figure 7 Bored echinoderm grain with subhedral overgrowth of non-ferroan calcite. Note adjacent pyrite-rich grains which are partially enclosed by rim cement. Sample 370-32-2, 52-55 cm, stained with Alizarin red-S and potassium ferricyanide. Plain light.

PLATE 3

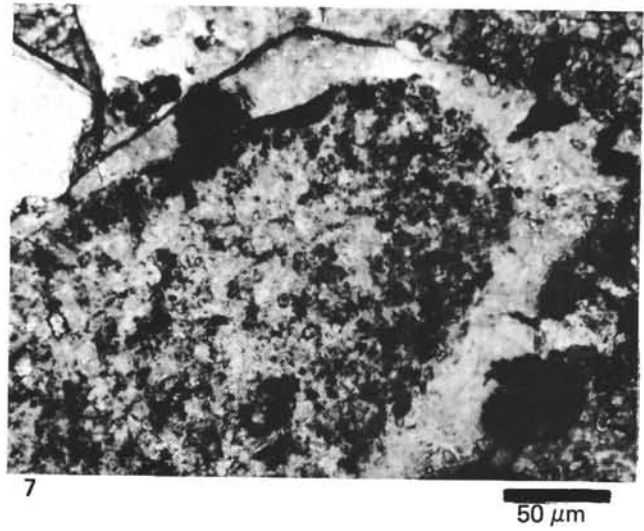
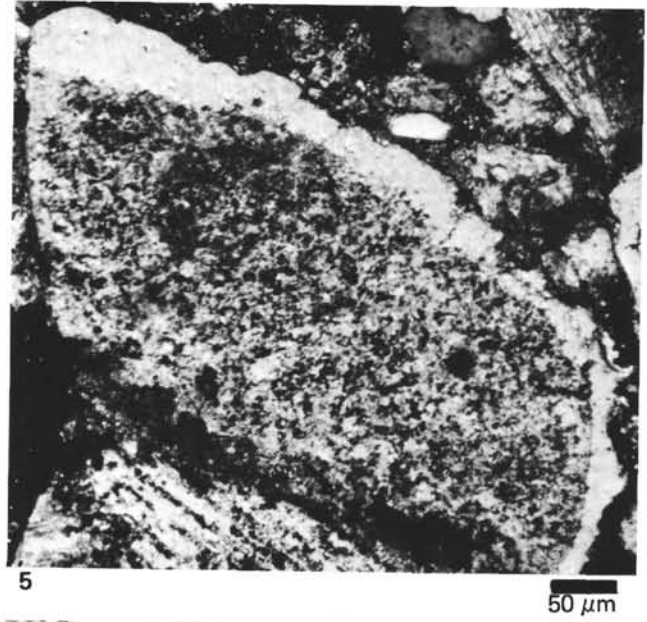
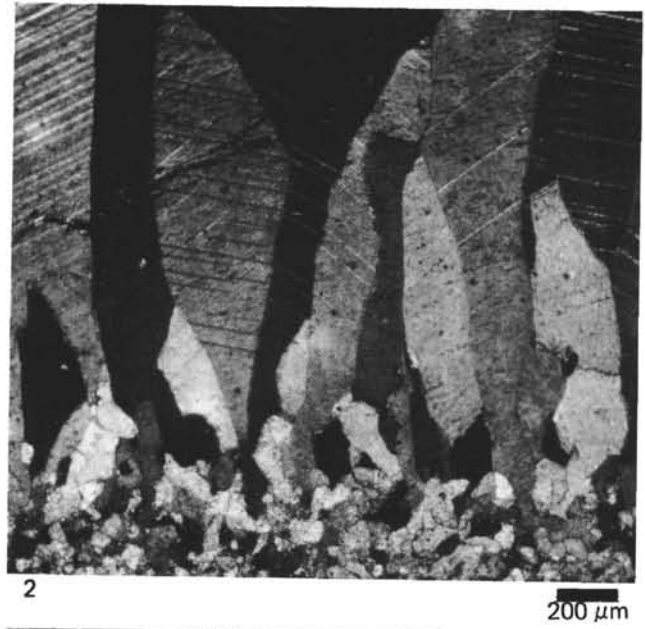
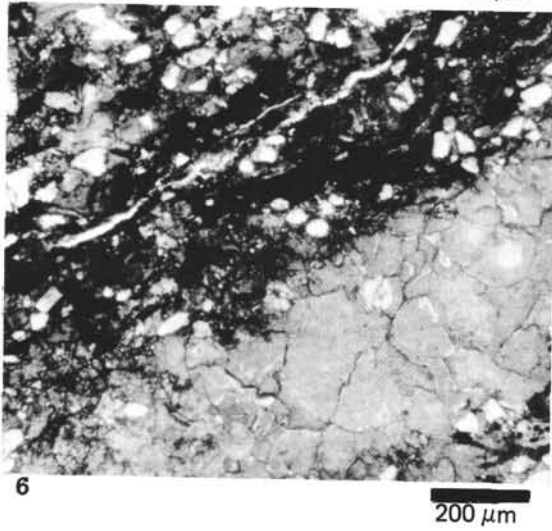
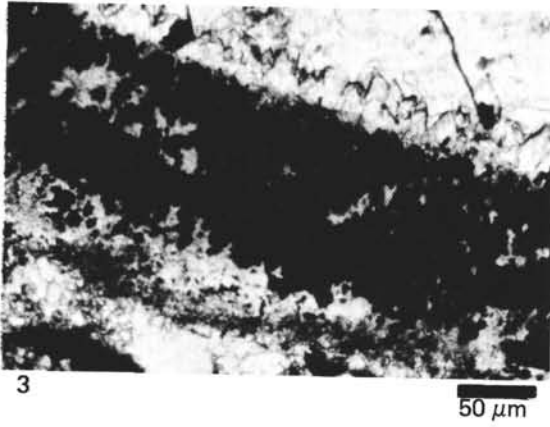
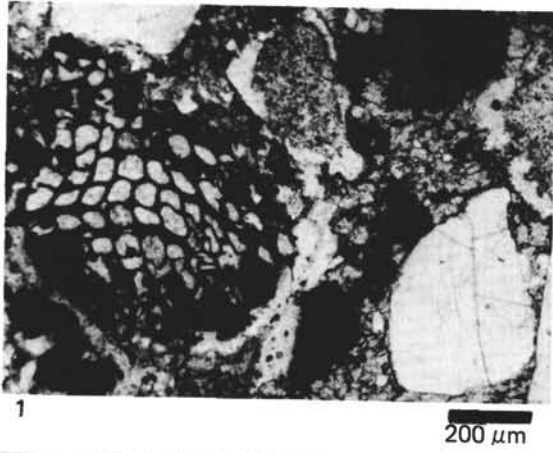


PLATE 4

SEM photomicrographs of microfabrics and diagenetic textures of limestones from Site 370, Cores 32 and 34.

- Figure 1 Terrigenous quartz grains in contact with sparry interparticle cement. Note micromorphology of large quartz grain and faceted surface of small quartz grain. Sample 370-34-1, 77-79 cm.
- Figure 2 Oriented subhedral crystals of interstitial spar. Note tiny carbonate rhombs (?dolomite). Sample 370-34-1, 68-71 cm.
- Figure 3 Interlocked rhombohedral crystals of ferroan ?high-Mg calcite forming interparticle cement. Notice significant intercrystal porosity. Sample 370-32-4, 86-89 cm.
- Figure 4 Euhedral ferroan high-Mg calcite crystals partially overgrown by zeolitic minerals. Sample 370-32-4, 86-89 cm.
- Figure 5 Fracture surface of calcite cement in contact with quartz grain. Sample 370-34-1, 68-71 cm.
- Figure 6 Enlargement of Figure 5. Note also micromorphology of quartz surface. Sample 370-34-1, 68-71 cm.

PLATE 4

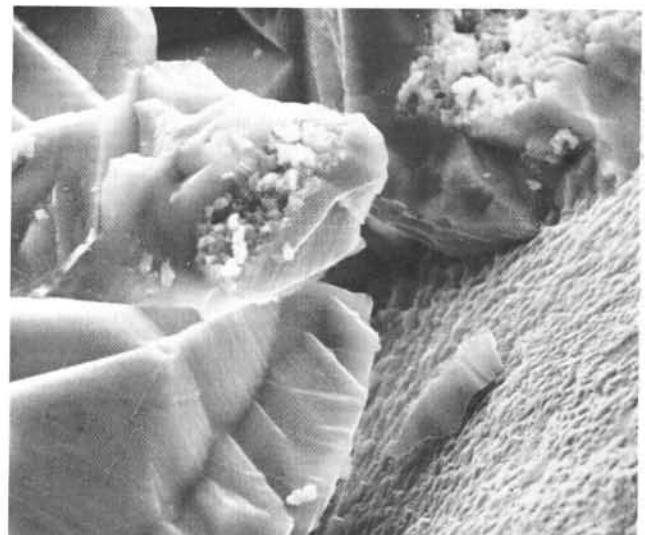
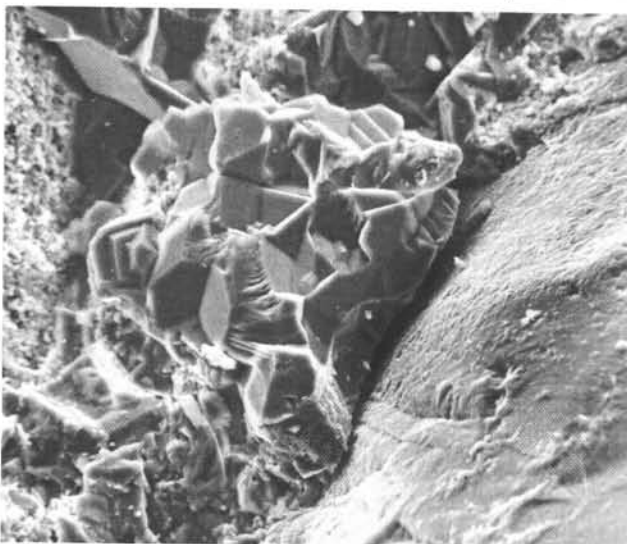
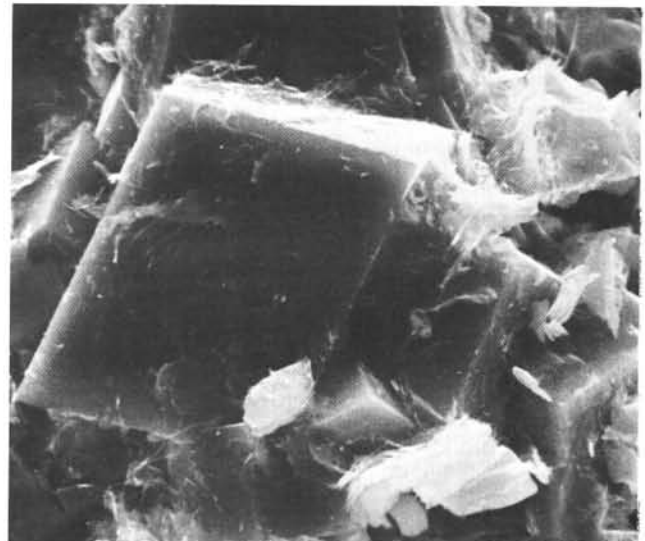
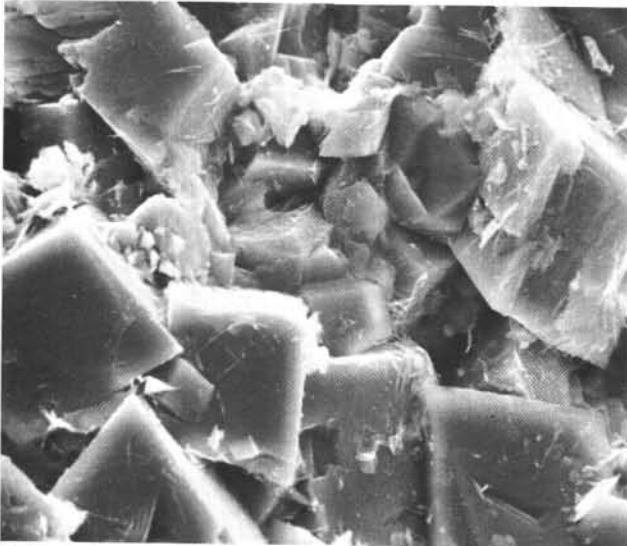
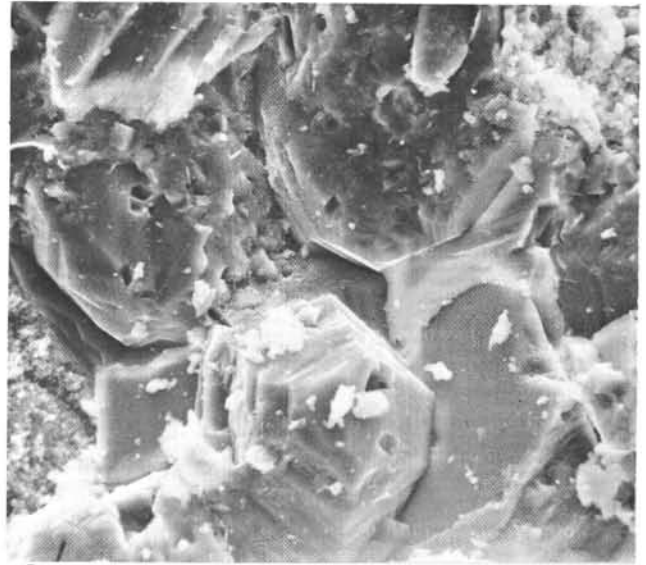
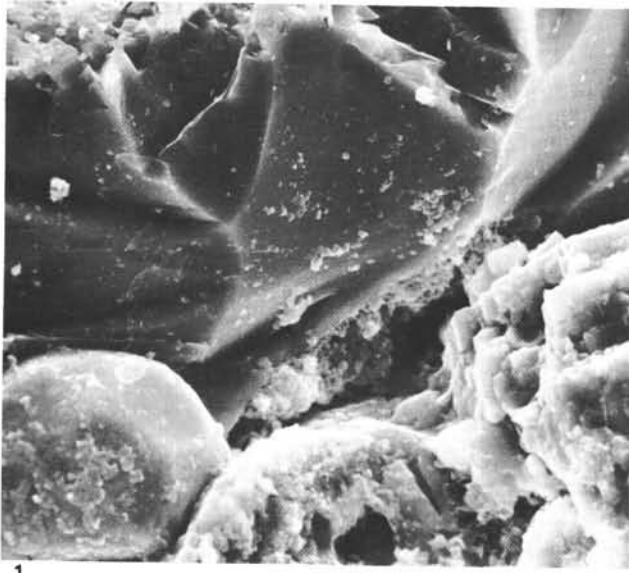
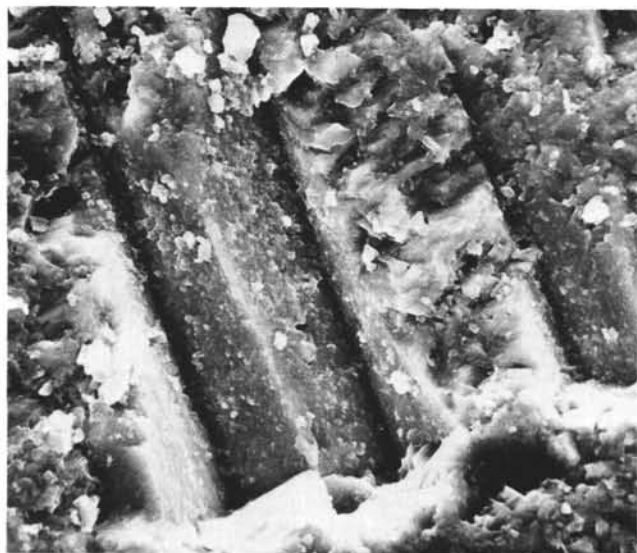


PLATE 5

SEM photomicrographs of microfabrics and diagenetic textures of limestones from Site 370, Cores 32 and 34.

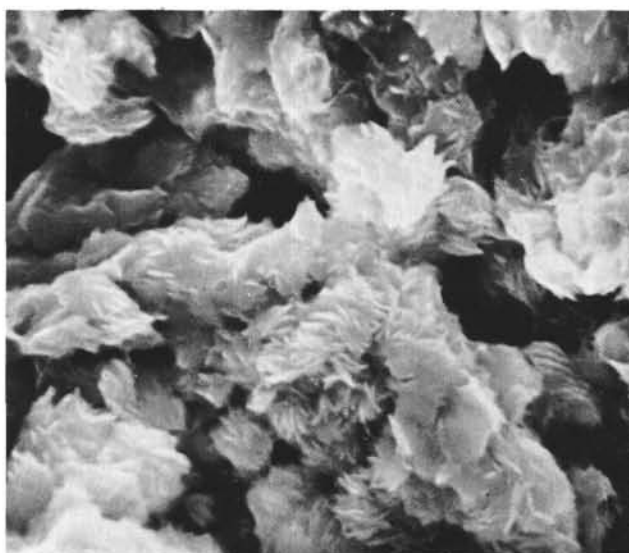
- Figure 1 Fracture surface of molluscan shell fragment (?Pinnacea) showing well-preserved calcite of prismatic layer. Sample 370-34-1, 46-48 cm.
- Figure 2 Aggregates of late authigenic mineral (?zeolites) grown in intercrystal pore space. Sample 370-32-4, 86-89 cm.
- Figure 3 Spherules of framboidal pyrite filling intercrystal pores. Sample 370-32-4, 86-89 cm.
- Figure 4 Micron-sized authigenic pyrite crystals grown upon well-developed crystal surfaces of second-generation calcite cement. Sample 370-32-4, 86-89 cm.
- Figure 5 Polished section of cemented limestone showing grain-to-grain relations of elongated carbonate grains coated by calcite and subangular quartz grain. Interstitial pore in the center is filled with low-Mg calcite. Sample 370-34-1, 46-48 cm.
- Figure 6 Smoothed fracture surface of oölite showing rounded calcitic grain as nucleus and concentric layers of the coating. Sample 370-34-1, 68-71 cm.

PLATE 5



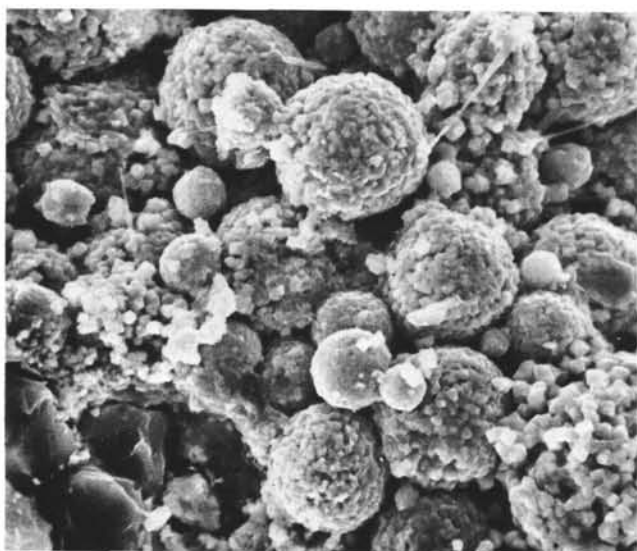
1

10  $\mu\text{m}$



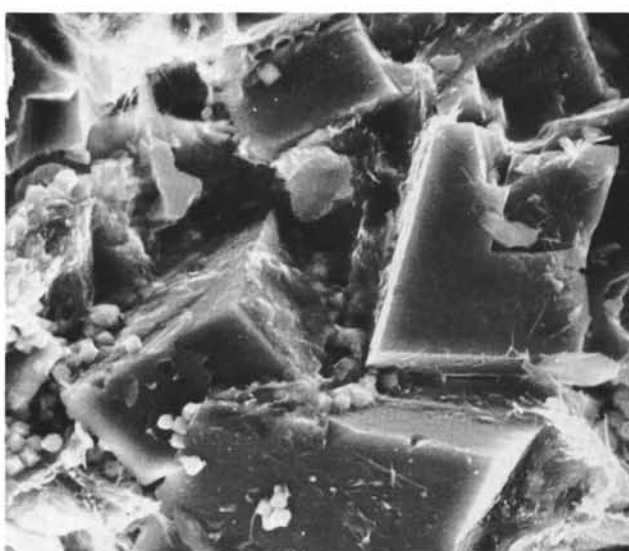
2

2  $\mu\text{m}$



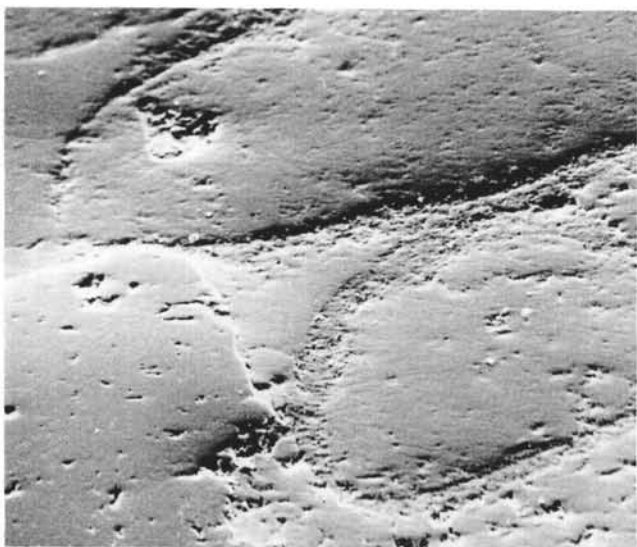
3

10  $\mu\text{m}$



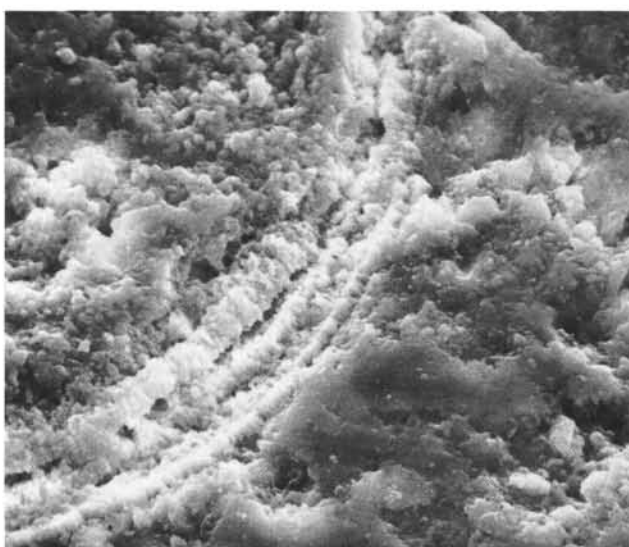
4

5  $\mu\text{m}$



5

25  $\mu\text{m}$



6

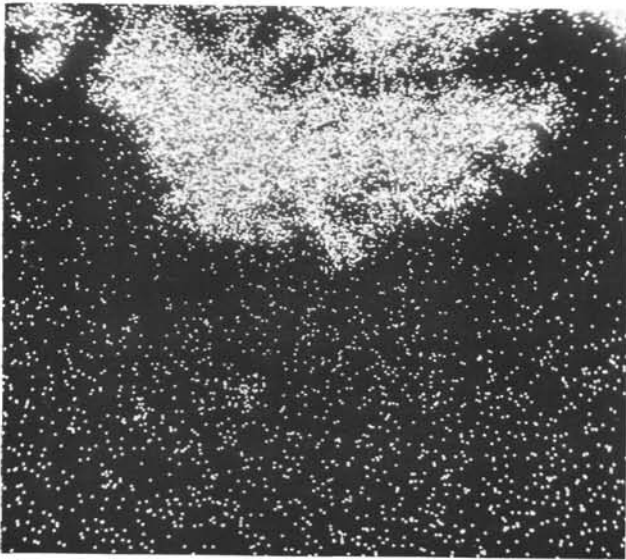
10  $\mu\text{m}$

PLATE 6

Element distribution maps of Site 370 carbonates.  
Sample 370-32-2, 52-55 cm.

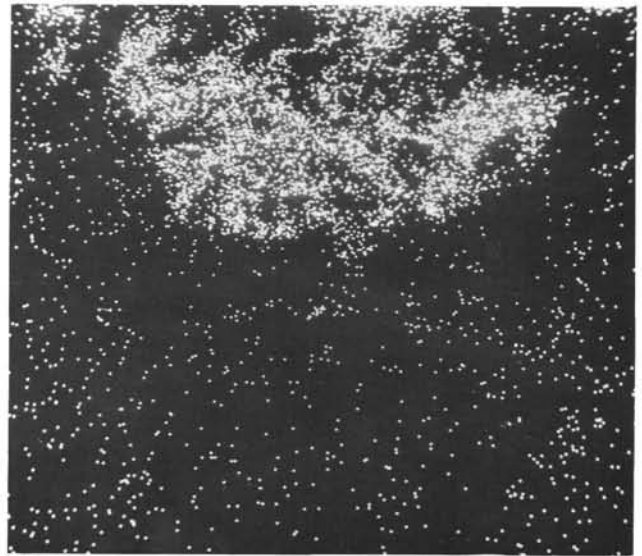
- Figure 1      Distribution of iron in the pyrite-bearing arenaceous limestone (microfacies B). Compare Figures 2-4 of congruent section.
- Figure 2      Distribution of sulfur indicating pyrite concentration (see Figure 1).
- Figure 3      Distribution of calcium corresponding to the distribution of carbonate grains (calcite) and sparry cement.
- Figure 4      Distribution of aluminum of partially disintegrated potassium feldspar.
- Figure 5      Pyrite-rich section (different from Figures 1-4) showing element distribution of iron (compare Figure 6). Notice that concentration of iron (indicating pyrite) partially follows bedding which is oriented horizontally.
- Figure 6      Distribution of calcium (see Figure 5).

PLATE 6



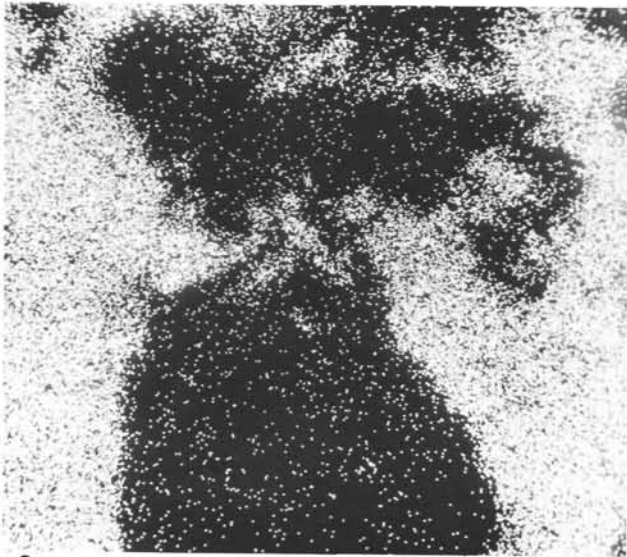
1

20  $\mu\text{m}$



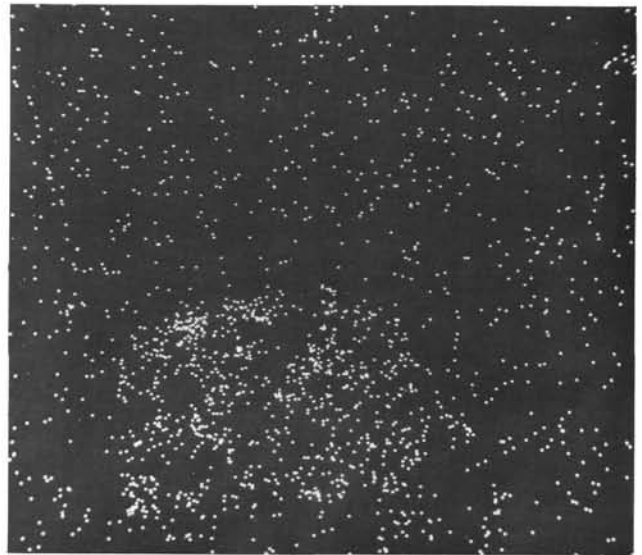
2

20  $\mu\text{m}$



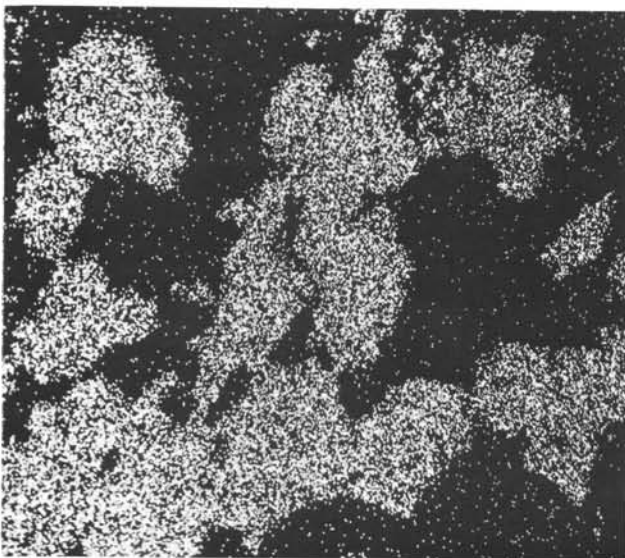
3

20  $\mu\text{m}$



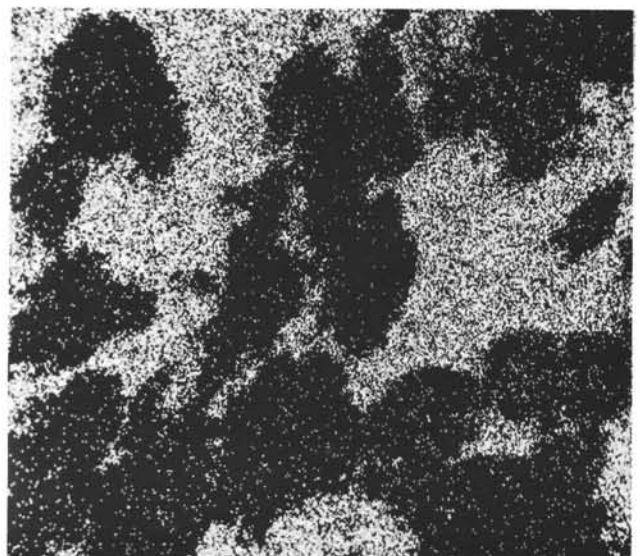
4

20  $\mu\text{m}$



5

100  $\mu\text{m}$



6

100  $\mu\text{m}$